Journal of Cell Science 112, 4601-4613 (1999)
Printed in Great Britain © The Company of Biologists Limited 1999
JCS0904

Identification of PA2.26 antigen as a novel cell-surface mucin-type glycoprotein that induces plasma membrane extensions and increased motility in keratinocytes

Francisco G. Scholl[1], Carlos Gamallo[2], Senén Vilaró[3] and Miguel Quintanilla[1,*]

[1]Instituto de Investigaciones Biomédicas Alberto Sols CSIC-UAM, 28029-Madrid and [2]Departamento de Anatomía Patológica, Hospital de la Princesa, Facultad de Medicina UAM, 28029-Madrid, Spain
[3]Departament de Biologia Cellular, Universitat de Barcelona, 08028-Barcelona, Spain
*Author for correspondence (e-mail: mquintanilla@iib.uam.es)

Accepted 1 October; published on WWW 30 November 1999

SUMMARY

PA2.26 antigen was identified as a cell-surface protein induced in epidermal carcinogenesis and skin remodeling processes. PA2.26 is expressed in carcinoma cell lines and cultured fibroblasts but absent in nontumorigenic keratinocytes. In tissues, PA2.26 is present in epithelial cells of the choroid plexus, ependyma, glomerulus and alveolus, in mesothelial cells, and in endothelia of lymphatic vessels. Biochemical characterization of PA2.26 protein and sequence analysis of the isolated cDNA demonstrate that PA2.26 antigen is a mucin-like transmembrane glycoprotein. Confocal and immunoelectron microscopy analysis in cultured cells reveal that PA2.26 is concentrated in actin-rich microvilli and plasma membrane projections, such as filopodia, lamellipodia and ruffles, where it colocalizes with members of the ERM (ezrin, radixin, moesin) family protein. Ezrin and moesin, but not radixin, can be coimmunoprecipitated together with PA2.26 from cell lysates. Ectopic expression of PA2.26 in immortalized, nontumorigenic, keratinocytes induces an epithelial-fibroblastoid morphological conversion with increased plasma membrane extensions, concomitantly to a major reorganization of the actin cytoskeleton, redistribution of ezrin to cell-surface projections, and enhanced motility. These findings suggest an involvement of PA2.26 in cell migration.

Key words: PA2.26, Membrane extension, Actin, Ezrin, Motility

INTRODUCTION

Glycoproteins are involved in many cellular activities, in embryogenesis and development, and are particularly important in diseases such as cancer (Brockhausen et al., 1998). They contain oligosaccharides based on N-acetylgalactosamine (GalNAc) α-linked to serine or threonine (O-glycans) and N-acetylglucosamine (GlcNAc) β-linked to asparagine (N-glycans). Mucins are characterized by an extremely high content of O-glycans and are subdivided in secretory and membrane-associated forms (Gendler and Spicer, 1995). Mucin-like transmembrane glycoproteins have been found in epithelial and nonepithelial tissues, and can fulfill a protective role from environmental agents as well as other biological activities. For example, several membrane-associated mucins are involved in cell-cell interactions and mediate leukocyte trafficking, thrombosis and inflammation (Hilkens et al., 1992; Varki, 1994; Gendler and Spicer, 1995).

Cancer cells commonly exhibit changes in the expression of cell-surface mucins or their carbohydrate epitope exposure that are detected by specific monoclonal antibodies (mAbs) (Brockhausen et al., 1998). These mucins act as anti-adhesive molecules due to their large rod-like extracellular domains and are thought to mediate invasion and metastasis when overexpressed in carcinoma cells (Kemperman et al., 1994; Wesseling et al., 1995; Komatsu et al., 1997).

In a previous work, we described a cell-surface antigen of about 45 kDa, detected by mAb PA2.26, which is induced in keratinocytes during mouse epidermal carcinogenesis. PA2.26 antigen is absent from cultured nontumorigenic keratinocytes and from the normal mouse epidermis but it is expressed by squamous and spindle carcinoma cell lines, and in tumors produced in vivo by chemical carcinogenesis. Interestingly, the antigen is also present in cultured fibroblasts and stromal cells of the tumors, and it is induced in the skin during tissue regeneration after wounding and treatment with the tumor promoter phorbol 12-myristate 13-acetate (PMA) (Gandarillas et al., 1997).

In this study, we have defined the localization of PA2.26 protein in cultured cells and tissues, and examined its relationship with the actin cytoskeleton and members of the ERM (ezrin, radixin, moesin) family protein. Purification of the antigen by affinity chromatography and peptide sequencing allowed us to clone the mouse cDNA encoding PA2.26.

Sequence analysis of the isolated cDNA, as well as biochemical characterization of the immunoprecipitated protein, identified PA2.26 as a small mucin-like transmembrane glycoprotein of 172 amino acids. In an effort to gain insights into the function of PA2.26, we have transfected its cDNA into immortalized keratinocytes which do not express the antigen. Expression of PA2.26 in these cells induces a dramatic reorganization of the actin cytoskeleton and a redistribution of ezrin, concomitantly to a change in cell morphology from epithelial to fibroblastoid. The PA2.26-expressing cells acquired migratory properties.

MATERIALS AND METHODS

Cell lines and antibodies

The origins of nontumorigenic MCA3D keratinocytes and mouse carcinoma cell lines, PDV, HaCa4 and Car C, have been described elsewhere (Gandarillas et al., 1997). The human keratinocyte cell line HaCaT (Boukamp et al., 1988) was kindly provided by Dr Norbert Fusenig (German Cancer Research Center, Heidelberg, Germany). Cells were grown in Ham's F-12 medium supplemented with amino acids, 10% foetal calf serum and antibiotics (2.5 μg/ml amphotericin B, 100 μg/ml ampicillin, and 32 μg/ml gentamicin; Sigma Chemical Co., St Louis, MO). Mouse fibroblast cell lines NIH3T3 and Swiss 3T3, and HaCaT keratinocytes, were grown in Dulbecco's modified Eagle's medium containing 10% foetal calf serum and antibiotics. Cells were maintained on plastic in a humidified, 5% CO_2 atmosphere, at 37°C.

The rat IgG2a mAb PA2.26 was generated in our laboratory by immunization with whole suspended PDV cells, as previously described (Gandarillas et al., 1997). Rabbit anti-ezrin, anti-radixin and anti-moesin polyclonal antibodies were a kind gift from Dr Paul Mangeat (University of Montpellier, Montpellier, France). The mouse mAb 3C12 against ezrin was a gift from Dr Ossi Turunen (University of Helsinki, Helsinki, Finland).

Immunoprecipitation and western blot

Cultured cells were lysed in buffer A (1% Triton X-100, 10 mM Hepes, pH 6.8, 100 mM NaCl, 2.5 mM $MgCl_2$, 2 mM EGTA) or, when indicated, in RIPA buffer (0.1% SDS, 0.5% sodium deoxycholate, 1% Nonidet P-40, 150 mM NaCl, 50 mM Tris-HCl, pH 8.0), and a cocktail of protease inhibitors (1 mM phenylmethylsulfonyl fluoride, 5 μg/ml aprotinin and 5 μg/ml leupeptin) for 15 minutes at 4°C. The lysates were precleared with rat IgG covalently coupled to CNBr-activated Sepharose 4B (Pharmacia Biotech AB, Uppsala, Sweden), and then immunoprecipitated with mAb PA2.26-Sepharose 4B for 1 hour at 4°C. Immunocomplexes were washed three times in lysis buffer, eluted by boiling in 10 mM Hepes, pH 6.8, 100 mM NaCl, 2 mM EGTA, 2% SDS, for 5 minutes, and resolved by SDS-PAGE.

After electrophoresis, proteins were transferred from gels to Immobilon P membranes (Millipore Corp., Bedford, MA). The filters were exposed to primary antibodies and secondary antibodies coupled to horseradish peroxidase; Amersham Corp., Arlington Heights, FL). The peroxidase activity was developed by using an enhanced chemiluminescence kit (ECL; Amersham Corp.).

Triton X-114 phase separation and phosphatidylinositol-phospholipase C treatments

PDV cells were homogenized in a buffer containing 10 mM Hepes, pH 6.8, 100 mM NaCl, 2.5 mM $MgCl_2$, 2 mM EGTA, 0.3 M sucrose, and clarified by centrifugation. The supernatant was centrifuged at 90000 ***g*** for 30 minutes, and the pellet containing the membrane fraction extracted with Triton X-114 followed by temperature-induced phase separation, as reported (Bordier, 1981).

For treatment with phosphatidylinositol-phospholipase C (PI-PLC), subconfluent PDV cultures were cell-surface radiolabeled with carrier-free ^{125}I (Amersham Corp.), as previously described (Gandarillas et al., 1997). After labeling, cells were washed in PBS and incubated with 350 mU/ml of PI-PLC (Boehringer Mannheim) in serum-free medium for 1 hour at 37°C. As a control, labeled cells were incubated in medium alone. Culture media were collected, and cells lysed in buffer A plus protease inhibitors. PA2.26 was immunoprecipitated from the culture media and cell extracts as described above. The immunoprecipitates were resolved by 10% SDS-PAGE under reducing conditions and analyzed by autoradiography.

Lectin incubation and glycosidase digestions

For detection of glucidic residues, the following digoxigenin-labeled lectins (Boehringer Mannheim, Mannheim, Germany) were used: *Datura stramonium* (DSA), *Galanthus nivalis* (GNA), *Maackia amurensis* (MAA), *Sambucus nigra* (SNA), *Aleuria aurantia* (AAA) and *Arachis hypogea* (PNA). PA2.26 immunoprecipitates were resolved by 10% SDS-PAGE and transferred to Immobilon P membranes. Filters were incubated with digoxigenin-labeled lectins followed by anti-digoxigenin Fab fragments coupled to alkaline phosphatase, as specified by the manufacturer's recommendations.

For digestion of PA2.26 antigen with glycosidases, PA2.26 immunocomplexes were concentrated by cold acetone at −20°C. Pellets were solubilized in digestion buffer (30 μl) and treated with the following glycosidases: 1 U of N-glycosidase F (Boehringer Mannheim) in 20 mM phosphate buffer, pH 7.2, 5 mM EDTA, 0.5% Nonidet P-40; 20 mU of neuraminidase from *C. perfringens* (Sigma Chemical Co) in 50 mM acetate buffer, pH 5.5; 1 mU of O-glycosidase (Boehringer Mannheim) in 20 mM phosphate buffer, pH 6.0, 0.1% Triton X-100. Incubations were for 2 hours (neuraminidase) or overnight (N-glycosidase F, O-glycosidase) at 37°C.

Purification of PA2.26 antigen and amino acid sequence analysis

The membrane fraction of mouse brain extracts was used as the source of PA2.26 antigen. Collected brains were cut into several pieces and homogenized in ice-cold 20 mM Hepes, pH 7.2, plus protease inhibitors. The homogenate was passed through several pieces of gauze, layered on the top of a discontinuous 0.8 M and 1.2 M sucrose gradient, and centrifuged at 140000 ***g*** for 1 hour. The interface fraction was diluted in 20 mM Hepes, pH 7.2, centrifuged at 140000 ***g*** for 1 hour, and the pellet lysed in buffer A containing 0.1% SDS and protease inhibitors. The lysate was precleared by passing through a column of rat IgG-Sepharose 4B equilibrated in buffer A and then loaded onto a column of mAb PA2.26-Sepharose 4B previously equilibrated in buffer A. The column was washed sequentially with buffer A and buffer A containing 0.5 M NaCl, and PA2.26 antigen eluted with buffer B (10 mM Hepes, pH 6.8, 0.5 M NaCl, 1% SDS, 2 mM EGTA, 2.5 mM $MgCl_2$) after boiling the beads for 5 minutes. The supernatant was concentrated with cold acetone at −20°C, the pellet resuspended in buffer B and resolved in 10% SDS-PAGE (gel thickness, 0.75 mm) under nonreducing conditions. A single protein band migrating at 45 kDa (corresponding to the mature form of PA2.26 antigen) was excised from the Coomassie blue-stained gel, soaked in water and processed for internal peptide sequencing in Eurosequence (Groningen, The Netherlands).

RT-PCR and molecular cloning of PA2.26 antigen

Based on the sequence information of the *OTS-8* cDNA (Nose et al., 1990), two oligonucleotides were generated flanking the coding sequence of *OTS-8:* the sense primer 5′-AAAAACCCACTA-GCTGCTGAGGCTCCAA-3′ and the antisense primer 5′-ATGG-GTCATCTTCCTCCACAGGAAGAGG-3′. Reverse transcription was performed at 42°C for 1 hour using the enzyme from avian

myeloblastosis virus (Promega, Madison, WI), 100 ng of a poly(A)$^+$-enriched RNA fraction (Mini RiboSep; Becton Dickinson Labware, Bedford, MA) extracted from the cell lines, as templates, and random hexameres as primers. The products of the reactions were tenfold diluted and used for PCR (30 cycles: 94°C for 1 minute, 55°C for 2 minutes and 72°C for 3 minutes) in a Gene Amp PCR system 2400 (Perkin Elmer, Foster City, CA). The resulting 659 bp cDNA fragment was cloned into pGEM-t (Promega) and sequenced in both directions.

cDNA transfection

The cDNA coding for PA2.26 antigen was subcloned into the expression vector pcDNA3 (InVitrogen, San Diego, CA), downstream from the cytomegalovirus promoter.

For transient transfections, cells were seeded on glass coverslips 24 hours before DNA transfer. Cells were transfected using lipofectamine reagent (Gibco BRL, Gaithesburg, MD) and analyzed for immunofluorescence 36 hours after.

For stable transfection of MCA3D keratinocytes, cells cultured on plates were processed as mentioned above. Transfected cells were selected by growing in medium containing 0.4 mg/ml of G418 for 3-4 weeks, and individual clones isolated by cloning rings.

Infection/transfection experiments were performed as previously described (García-Gallo et al., 1999). Briefly, COS cells were infected with vTF7-3 virus at a multiplicity of four plaque-forming units per cell, for 1 hour at 37°C. After adsorption, virus inoculum was removed, cells were washed once in Dulbecco's modified Eagle's medium containing 2% foetal calf serum, and transfected using lipofectamine reagent.

Immunofluorescence microscopy

For single- and double-staining immunofluorescence microscopy analysis, cells grown on glass coverslips were fixed with 3.7% formaldehyde in PBS and permeabilized with 0.05% Triton X-100 for 10 minutes. Coverslips were soaked in PBS containing 1% BSA and incubated with the indicated antibodies for 1 hour at 37°C in a moist chamber. FITC-labeled goat anti-rat IgG or rhodamine-conjugated goat anti-rabbit IgG (Jackson, West Grove, PA) were used as secondary antibodies. For F-actin staining, phalloidin coupled to rhodamin compound was used. Coverslips were then mounted in mowiol and examined with a fluorescence microscope (Axiophot; Carl Zeiss, Oberkochen, Germany).

Confocal microscopy analysis was carried out as previously described (Pagan et al., 1996) in a confocal scanning laser microscope (TCS 4D; Leica Lasertechnik GmbH, Heidelberg, Germany) adapted to an inverted Leitz DMIRBE microscope equipped with a krypton/argon laser. From 14 serial optical sections for each fluorochrome, made through a depth of 7 μm inside the specimen (except for Fig. 9, in which four serial optical sections were made through a depth of 4 μm), a three-dimensional image was assembled using ImageSpace software.

Electron microscopy

PDV cells grown on Transwell chambers were fixed with 2% paraformaldehyde in phosphate buffer (PB) for 1 hour at 4°C. After washing in PB containing 20 mM glycine (PB-G), cells were incubated with 1% BSA in PB-G for 10 minutes at room temperature. Cells were stained with mAb PA2.26, followed by incubation with rabbit anti-rat IgG and 15-nm colloidal gold-labeled protein A (British Bio Cell, Cardiff, UK). Each of these incubations were in blocking solution for 1 hour at room temperature. Cells were post-fixed with 2% paraformaldehyde, 2.5% glutaraldehyde in PB buffer. The polycarbonate membrane was excised from the Transwell chamber, treated with 2% osmium tetroxide, dehydrated in ethanol and embedded in Spurr as previously described (Casaroli-Marano et al., 1998). Ultrathin sections (30-50 nm) were observed and photographied by conventional TEM (Hitachi 600 AB).

Immunohistochemistry

Organ specimens of adult mice were obtained, fixed in formalin and embedded in paraffin. Immunostaining for PA2.26 antigen was performed by the avidin-biotin-alkaline phosphatase method in deparaffinized sections after heat-induced antigen retrieval, as previously described (Palacios and Gamallo, 1998).

Migration assay

Confluent cell monolayers were gently scratched with a tip to produce a wound. Then, cultures were allowed to grow for 24 hours in the

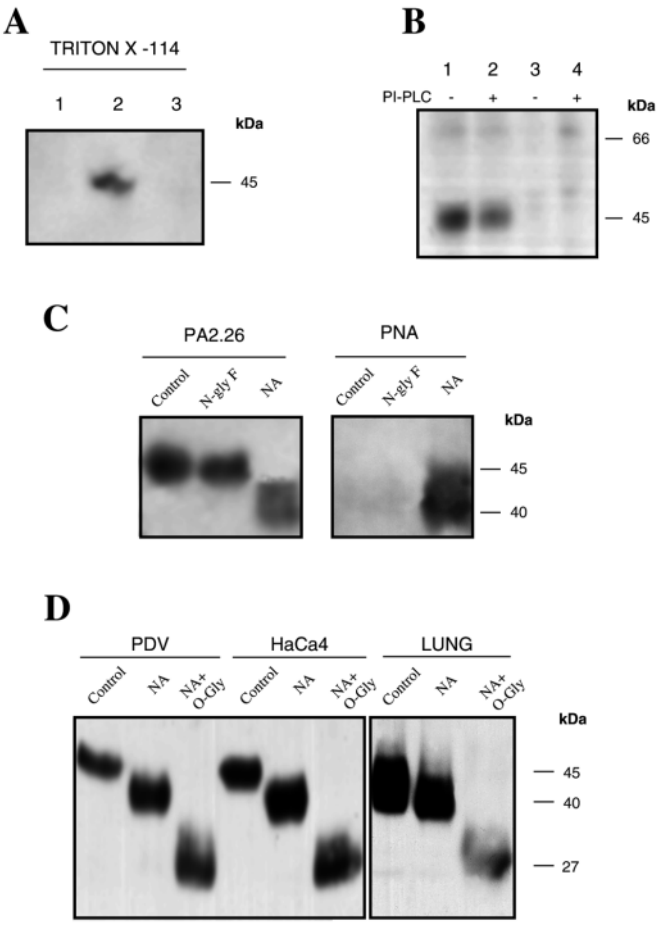

Fig. 1. Biochemical characterisation of PA2.26 antigen. (A) Phase separation of PA2.26 antigen. The membrane fraction of PDV cells was extracted with the detergent Triton X-114. After centrifugation, the pellet was solubilized in Laemmli buffer (lane 1) and the supernatant subjected to temperature-induced phase separation resulting in organic (lane 2) and aqueous (lane 3) phases. Samples corresponding to the same number of cells were run on 10% SDS-PAGE and immunoblotted with PA2.26 mAb. (B) Treatment with PI-PLC. ^{125}I-labeled PDV cells were incubated in culture medium alone (lanes 1 and 3) or in medium containing PI-PLC enzyme (lanes 2 and 4). The cell lysates (lanes 1 and 2) and culture media (lanes 3 and 4) were immunoprecipitated with mAb PA2.26 and resolved by 10% SDS-PAGE. (C,D) Analysis of glucidic composition of PA2.26 antigen. (C) PA2.26 immunoprecipitates from PDV cells were treated with N-glycosidase F (N-gly F), neuraminidase (NA) or buffer (Control). (D) PA2.26 immunoprecipitated from PDV, HaCa4 and lung extracts was incubated with NA, NA plus O-glycosidase (O-Gly) or buffer (Control). Samples were run on 10% SDS-PAGE and probed with PA2.26 mAb or PNA lectin. The positions of molecular mass markers are shown.

presence of medium plus serum. Cells invading the denuded area of the wounds were counted in 3-4 different fields from duplicates.

RESULTS

PA2.26 antigen is an integral mucin-like membrane protein

mAb PA2.26 recognizes a protein of about 45 kDa on the surface of mouse skin carcinoma cells (PDV, HaCa4, Car C) and cultured fibroblasts (NIH3T3, Swiss 3T3). To analyse the association of the antigen to the plasma membrane, the membrane fraction of PDV carcinoma cells was extracted with the detergent Triton X-114. After phase separation, hydrophilic proteins are found in the aqueous phase while integral membrane proteins with an amphiphilic nature are recovered in the detergent phase (Bordier, 1981). PA2.26 antigen was recovered in the organic phase (Fig. 1A, lane 2) and no detectable signal was observed neither in the insoluble fraction nor in the aqueous phase (Fig. 1A, lanes 1 and 3, respectively). Moreover, treatment of ^{125}I surface-labeled PDV cells with phosphatidylinositol-phospholipase C (PI-PLC) did not liberate the antigen into the culture medium (Fig. 1B), indicating that the protein is not attached to the membrane by a glycosil phosphatidylinositol anchor.

The broadness of the bands indicated that PA2.26 protein could be glycosylated. Therefore, we analysed the presence of specific carbohydrates using a set of digoxigenin-labeled lectins (Table 1). The intact antigen immunoprecipitated from PDV cells only bound MAA, indicating the presence of sialic acid (SA) linked α(2-3) to galactose, while it did not react with SNA, which also recognizes SA residues but α(2-6)-linked. Removal of SA residues by digestion with neuraminidase (NA) resulted in a shift in mobility from 45 kDa to 40 kDa and allowed binding of PNA, but not of other lectins, to the antigen (Fig. 1C, Table 1). PNA recognizes the unsubstituted disaccharide galactose β(1-3)N-acetylgalactosamine in O-glycans, and its positive reaction to neuraminidase-treated PA2.26 suggested the presence of O-linked carbohydrates in the protein. In fact, digestion of the desialylated antigen with O-glycosidase (O-Gly) yeld a further reduction of molecular mass to 27 kDa, as shown in Fig. 1D for PA2.26 immunoprecipitated from PDV and HaCa4 cell lines.

Table 1. Lectin binding analysis of immunoprecipitated PA2.26 antigen

			Binding to	
Lectin	Specificity	Chains recognized	Intact antigen	Antigen + NA
GNA	High mannose	N-glyc	–	–
SNA	SAα(2-6)-Gal	N- and O-glyc	–	–
MAA	SAα(2-3)-Gal	N- and O-glyc	+	–
PNA	Galβ(1-3)GalNAc	O-glyc	–	+
DSA	Galβ(1-4)GlcNAc	N- and O-glyc	–	–
AAA	Fuc	O-glyc	–	ND

Immunoprecipitated PA2.26 antigen was separated by SDS-PAGE before and after digestion with neuraminidase (NA) and blotted to Immobilon P. The blot was probed with the indicated lectins conjugated with digoxigenin and visualized with an anti-digoxigenin antibody coupled to alkaline phosphatase. SA, sialic acid; Gal, galactose; GalNAc, N-acetylgalactosamine; GlcNAc, N-acetylglucosamine; Fuc, fucose; ND, not determined.

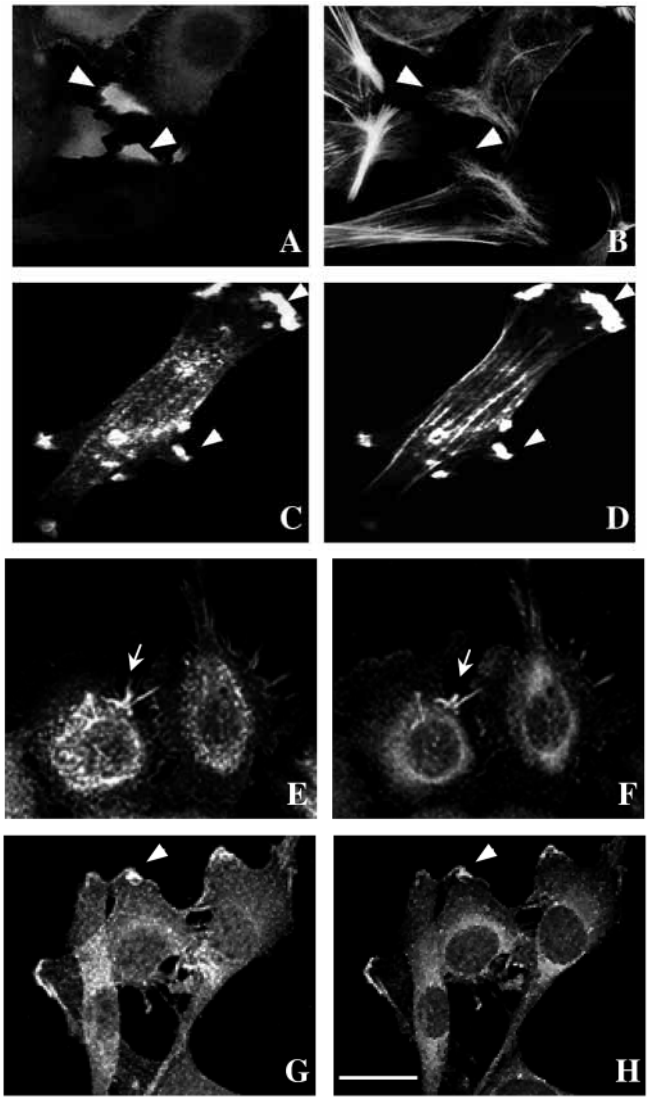

Fig. 2. Immunofluorescence colocalization of PA2.26 antigen with F-actin and ezrin in carcinoma and fibroblast cell lines.
(A-D) Colocalization of PA2.26 and F-actin in PDV (A,B) and Car C (C,D). Cells were doubly stained with PA2.26 mAb (A,C) and phalloidin (B,D). C and D show confocal images.
(E-H) Colocalization of PA2.26 and ezrin in PDV (E,F) and Swiss 3T3 (G,H) by confocal analysis. Cells were doubly stained with PA2.26 mAb (E,G) and an anti-ezrin polyclonal antibody (F,H). Arrowheads indicate lamellipodia and ruffles, and arrows filopodia. Bar, 10 μm.

Digestion with N-glycanase F (N-Gly F) did not change the mobility of the protein (Fig. 1C), indicating the absence, or minor presence, of N-linked sugars.

PA2.26 antigen is also expressed in normal mouse tissues such as brain and lung (see below). The protein recognized by the mAb PA2.26 in brain had a similar size, 45 kDa, to that detected in cultured cells (not shown), while the lung protein had a smaller molecular mass of about 42 kDa (Fig. 1D). This difference in size is likely due to a lesser degree of sialylation, as digestion of PA2.26 immunoprecipitated from lung extracts with neuraminidase shifted the mobility of the protein to 40 kDa and combined treatment with neuraminidase and O-

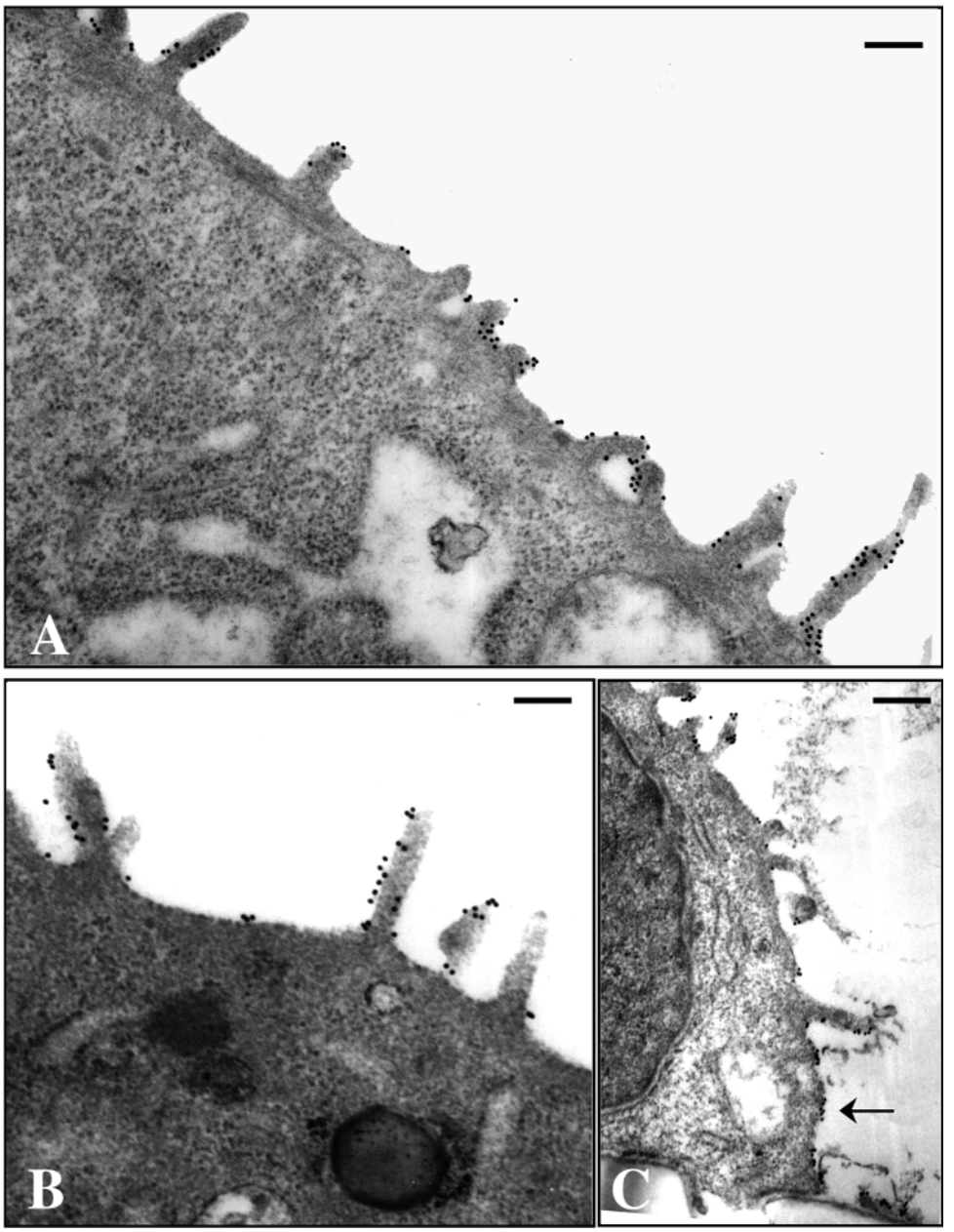

Fig. 3. (A-C) Immunoelectron microscopic localization of PA2.26 antigen at membrane microvilli of PDV cells. Arrow in (C) shows clusters of colloidal gold particles associated with planar regions of the membrane. Bars, 0.1 μm (A,B); 0.2 μm (C).

glycosidase again yielded a band of 27 kDa (Fig. 1D), as found above in cultured cells.

Overall, these data demonstrate that PA2.26 antigen is a highly glycosylated, mucin-like, integral membrane protein with an apparent peptide backbone of about 27 kDa.

PA2.26 antigen is located in actin-containing plasma membrane projections where it colocalizes with ERM proteins

Immunofluorescence analysis of PA2.26 in cultured cells revealed an intense staining in plasma membrane projections such as lamellipodia and ruffles (Fig. 2A,C,E,G). Double-staining fluorescence microscopy with mAb PA2.26 and phalloidin in PDV cells showed a colocalization of PA2.26 protein with actin filaments of lamellipodia and membrane projections from the leading edge, but the antigen seemed to be excluded from cortical actin bundles and stress fibers (Fig. 2A,B). These results were confirmed by confocal microscopy studies, as shown for the spindle carcinoma cell line Car C (Fig. 2C,D). These highly motile cells (Buchmann et al., 1991) exhibit prominent membrane ruffles rich in actin filaments (Fig. 2D), which were intensely stained with mAb PA2.26 (Fig. 2C). In addition, a punctate staining all along the cells located on the plasma membrane was also observed (see Fig. 2C). Similar results were obtained with NIH3T3 and Swiss 3T3 fibroblast cell lines (data not shown).

ERM proteins function as linkers between the actin cytoskeleton and the plasma membrane (see Tsukita et al., 1997; Mangeat et al., 1999, for reviews). They are concentrated at microvilli and other actin-rich surface structures in a wide variety of cells. Particularly, ezrin is found primarily in epithelial cells (Berryman et al., 1993). Therefore, we studied the possible colocalization of PA2.26 and ezrin in the cell lines by confocal microscopy (Fig. 2E-H). The pattern of ezrin staining in microvilli, membrane ruffles and lamellipodia was very similar to that seen for PA2.26 in PDV (Fig. 2E,F), and Swiss 3T3 cells (Fig. 2G,H). PA2.26 antigen also colocalized with moesin and radixin in these cultured cells, as demonstrated by double-staining immunofluorescence experiments (data not shown).

To examine the location of PA2.26 at the ultrastructural level, immunogold preembedding staining and electron microscopy studies were performed in PDV cells grown on Transwell chambers to preserve cell polarity (Fig. 3). PA2.26 protein was highly concentrated over membrane microvilli. Gold particles were distributed all along their surfaces (Fig. 3A,B), and only a minor fraction of gold particles appeared as clusters in planar regions of the plasma membrane (see arrow in Fig. 3C). No staining was observed on the basal membrane in contact with the substratum (Fig. 3C).

To analyse whether the antigen and ERM proteins associate in the cells, PA2.26 was immunoprecipitated from PDV lysates and the presence of ezrin, radixin and moesin assessed by western immunoblotting with specific antibodies (Fig. 4). In parallel, we carried out the same analysis with MCA3D cells, which do not express the antigen, as a control. Both MCA3D and PDV cell lines synthesize the three proteins of the ERM

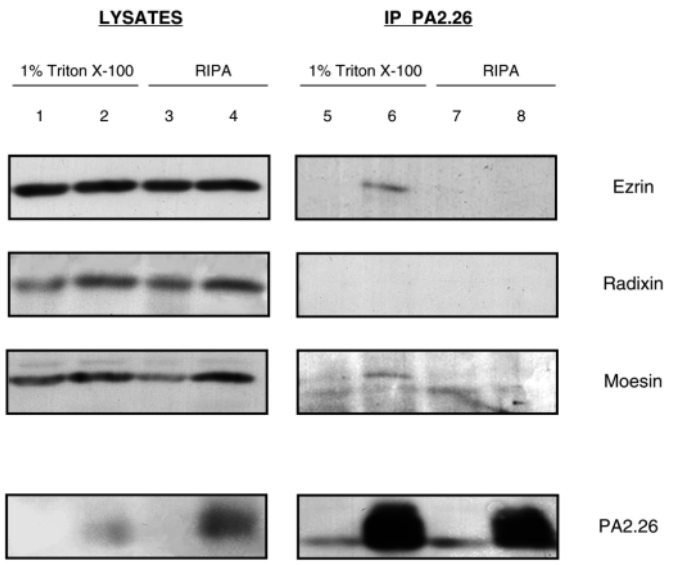

Fig. 4. Coimmunoprecipitation of ezrin and moesin with PA2.26 antigen. MCA3D (lanes 1, 3, 5 and 7) and PDV (lanes 2, 4, 6 and 8) cells were lysed in a buffer containing 1% Triton X-100 (lanes 1, 2, 5 and 6) or buffer RIPA (lanes 3, 4, 7 and 8). The presence of ERM proteins and PA2.26 antigen was determined in the lysates by western immunoblotting with anti-ezrin 3C12 mAb, anti-radixin and anti-moesin polyclonal antibodies, and PA2.26 mAb (lanes 1-4). Lysates were immunoprecipitated with PA2.26 mAb and the immunocomplexes resolved by 7.5% SDS-PAGE and immunoblotted with the above antibodies (lanes 5-8). Bands in lanes 5 and 7 of the lower panel correspond to the heavy chain of immunoglobulin.

family, as found by western analysis of cell lysates (Fig. 4, lanes 1-4). Protein bands corresponding to ezrin and moesin, but not radixin, could be detected in the PA2.26 immunoprecipitates from PDV cells lysed in 1% Triton X-100 (Fig. 4, lane 6). However, when cells were lysed in RIPA buffer neither ezrin nor moesin were present in the immunoprecipitates (Fig. 4, lane 8).

Distribution of PA2.26 protein in tissues

The expression of PA2.26 was examined in different mouse tissues by western immunoblotting. The protein was present at relatively high levels in lung and brain, and to a lesser extent in kidney, stomach, liver and oesophagus. No significant expression was found in skin, muscle and small intestine (data not shown).

Immunohistochemical staining in tissue sections revealed the presence of PA2.26 in different types of cells (Fig. 5). In the lung, the alveolar epithelium was intensely stained, while epithelial cells of the terminal bronchiole were negative (Fig. 5A). The choroid plexuses and ependymal epithelia expressed PA2.26 located at microvilli facing the ventricular cavity (Fig. 5B,C). All pleural, pericardial and peritoneal mesothelia examined were also positive with PA2.26 concentrated on the apical cell surface (see Fig. 5D,F). Endothelial cells from veins, arteries and endocardium were not stained (Fig. 5A,E,F,F′) and, surprisingly, the only positive endothelial cells were sited in the lymphatic capillaries, as can be observed in the small intestine (Fig. 5D) and liver (Fig. 5E). Noteworthy, cells of the intestinal mucosa did not express PA2.26 (Fig. 5D), nor did smooth muscle (Fig. 5D), skeletal (not shown) and cardiac (Fig. 5F,F′) cells. In the kidney, PA2.26 was found in podocyte cells of the glomeruli (Fig. 5G) and in the parietal epithelial cells of Bowman's capsule (not shown).

Identification and cloning of PA2.26 antigen

PA2.26 antigen was purified by affinity chromatography from the membrane fraction of mouse brain extracts, as described in Materials and Methods. A single band of 45 kDa corresponding to PA2.26 was obtained in the final eluate, and its area excised from the gel and processed for internal peptide sequencing. Two major peptides of 8 and 7 amino acids were separated by reverse-phase HPLC after tryptic digestion of the protein, and their amino acid sequences determined by Edman degradation (Fig. 6A). A search in the EMBL data base identified two mouse proteins, OTS-8 and gp38, containing amino acid sequences that matched that of the peptides (Fig. 6A). *OTS-8* was isolated as a PMA-inducible gene from an osteoblastic cell line (Nose et al., 1990) and *gp38* was cloned from thymus epithelial cells (Farr et al., 1992). Several differences due to single nucleotide changes could be observed on comparing the predicted amino acid sequences of both cDNAs. The main change was a T nucleotide at the 3′ end of the *gp38* sequence, absent in the *OTS-8* cDNA, that shifted the stop codon position such that the deduced cytoplasmic domain of the OTS-8 protein is 32 residues longer than that of gp38.

Appropiate 5′ and 3′ oligonucleotides flanking the open reading frame of the *OTS-8* cDNA were synthesized and used for RT-PCR experiments. A band of 659 bp was amplified using poly(A)$^+$ RNA from PDV, HaCa4 and NIH3T3 cell lines (Fig. 6B, lanes 2, 3 and 4, respectively), while no mRNA could be detected in MCA3D cells (Fig. 6B, lane 1). These data confirm our early assumption that PA2.26 antigen is not expressed in nontumorigenic MCA3D keratinocytes, as mAb PA2.26 was unreactive in this cell line (Gandarillas et al., 1997). The PDV RT-PCR-amplified cDNA fragment was cloned and sequenced (Fig. 6C). The sequence was almost identical to that reported for *OTS-8* cDNA (Nose et al., 1990), the only difference being a single T nucleotide insertion at position 547 that results in a change of frame from amino acid 170 and originates a stop codon at position 555 giving rise to a shorter C-terminal end, as occurred with *gp38* (Farr et al., 1992). The PDV cloned cDNA encoded a protein of 172 amino acids that included the two microsequenced peptides (underlined). It contains an N-terminal signal sequence with a putative cleavage site between amino acids 22 and 23. The mature protein has a predicted molecular mass of 18.2 kDa. A presumptive membrane-spanning domain (residues 135-163, shaded) is located near the C terminus followed by a short cytoplasmic tail of only 9 amino acids. A serine within this latter domain at position 167 is part of a potential cAMP and protein kinase C-dependent phosphorylation site. The extracellular domain contains only a putative N-glycosylation site at position 60 whereas potential O-glycosylation serine or threonine residues are very abundant. These data are in agreement with PA2.26 antigen being a type-I membrane mucin-like protein.

To confirm that this sequence encoded PA2.26 antigen, COS cells were infected with high multiplicity of the recombinant vTF7-3 virus and transfected with the PDV cDNA cloned in the pcDNA3 vector, to allow maximal expression of the protein. The mAb PA2.26 detected in western blots a doublet

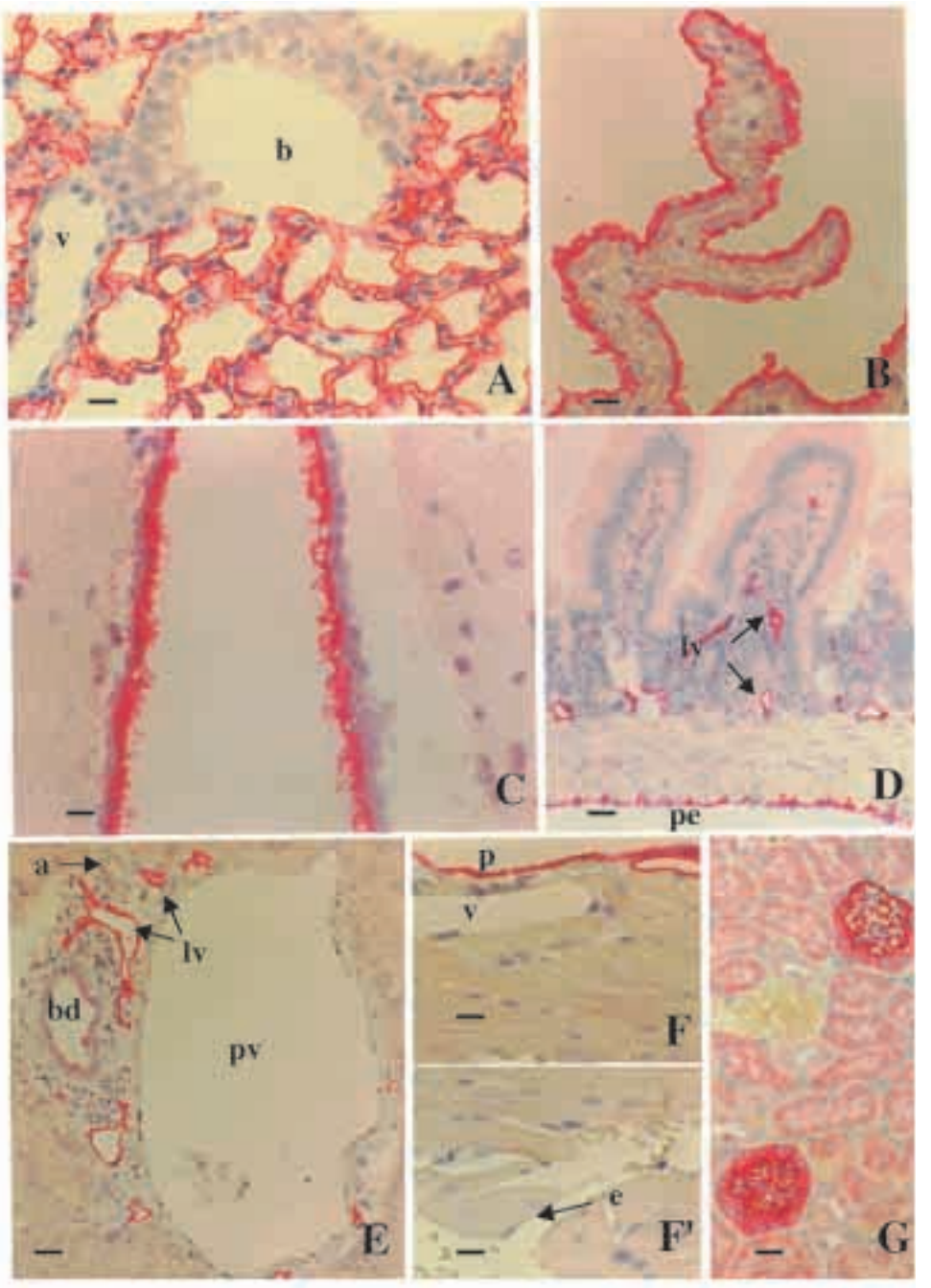

Fig. 5. Immunohistochemical localization of PA2.26 antigen in tissue sections. (A) lung; (B) choroid plexus; (C) ependymum; (D) small intestine; (E) liver; (F,F′) heart; (G) kidney. Intense staining is found in the epithelia of alveoli (A), choroid plexuses (B), ependyma (C) and glomeruli (G), in lymphatic vessel (lv) endothelia, and peritoneal (pe) and pericardial (p) mesothelia (see D-F). Some cells of the biliar ducts (bd) are also weakly stained in E. No staining is found in endothelial cells of the endocardium (e, see F′), portal vein (pv) and other veins (v) and arteries (a), nor in smooth (D) and cardiac (F,F′) muscle cells, or in cells of the intestinal mucosa (D) and kidney tubules (G; the background staining seen in this section is due to endogenous biotin). Note that PA2.26 antigen is clearly located at the plasma membrane (A) and microvillous projections (B,C). Bar, 10 μm (A-C, F,F′), 20 μm (D,E,G).

of 27 kDa corresponding to the core protein, an intermediate species of 30 kDa, and the mature glycosylated form of 45 kDa (Fig. 7, left panel). Similar results were obtained in infected/transfected MCA3D cells (data not shown). Immunofluorescence analysis in COS cells, and in immortalized mouse MCA3D and human HaCaT keratinocytes, transiently transfected with the PA2.26 cDNA, localized the antigen concentrated at ruffles, lamellipodia and microvilli (Fig. 7A-D). Some keratinocytes expressing PA2.26 antigen seemed to acquire a motile phenotype with increased membrane ruffling activity and formation of a leading edge in which the antigen was present (see Fig. 7C).

Transfection of PA2.26 antigen into MCA3D keratinocytes induces a change in morphology concomitantly to a reorganization of the actin cytoskeleton and increased motility

To study further the effect of PA2.26 antigen on the phenotype of keratinocytes, we obtained stable transfectants of MCA3D cells. Ten clones were selected and the expression of PA2.26 analysed by northern and western blots. All the transfectants expressed a mRNA of around 1.2 kb (Fig. 8A, lanes 3-12), absent in cells transfected with the empty vector (Fig. 8A, lane 2). Transformed PDV and HaCa4 keratinocytes expressed one species of RNA of 1.9 kb corresponding to the endogenous PA2.26 mRNA (Fig. 8A, lanes 13, 14). Low levels of PA2.26 protein expression were found in the transfectants when compared with NIH3T3 fibroblasts (Fig. 8B, compare lanes 2-7 with lane 8) or transformed keratinocytes (not shown). mAb PA2.26 recognized in the lysates a protein of 40 kDa in addition to the 45 kDa form (Fig. 8B, lanes 2-7). This protein of lower molecular mass is likely to represent an incompletely glycosylated antigen since immunoprecipitates from biotin-labeled cell surface transfectant clones contained only the mature form of 45 kDa (data not shown).

Expression of PA2.26 antigen in MCA3D keratinocytes induced a dramatic change in cell morphology (Fig. 8C). Parental MCA3D cells and control clones grew as islands with strong cell-cell contacts, exhibiting the typical paving stone appearance of epidermal keratinocytes at confluence (Fig. 8C, left). In contrast, PA2.26 transfectants showed an elongated morphology with numerous membrane protrusions, and were unable to grow as colonies of cohesive cells even at high cell

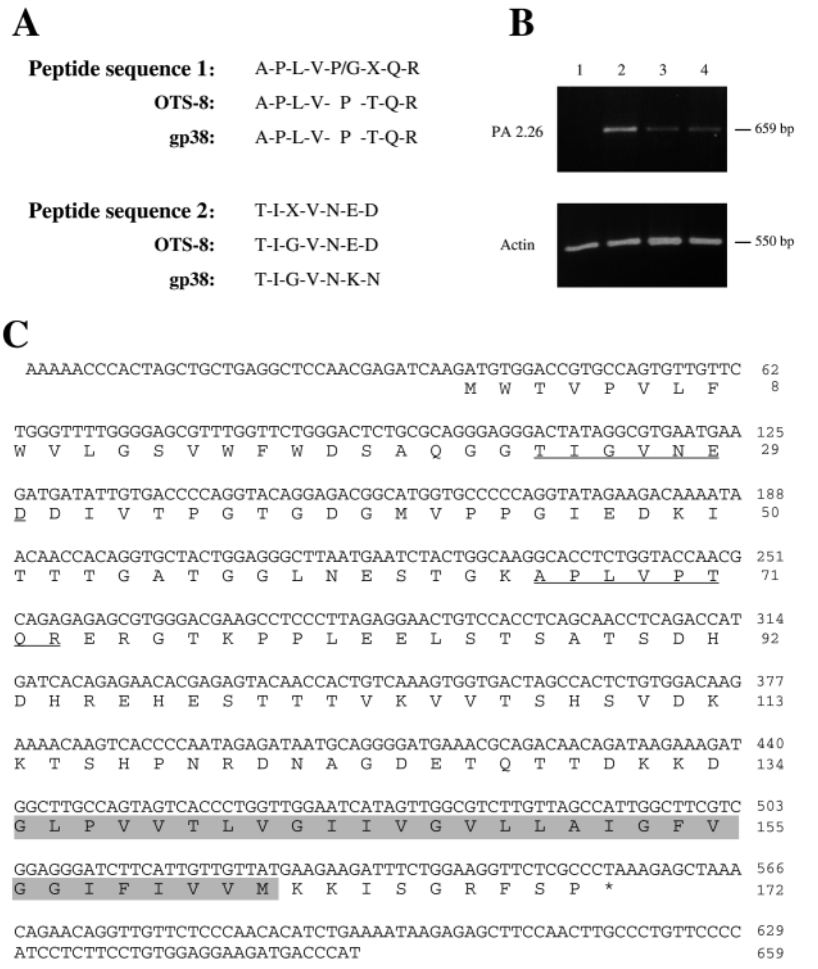

Fig. 6. Molecular cloning of PA2.26 cDNA. (A) Amino acid sequences of two peptides obtained from the purified antigen showing homologies with OTS-8/gp38 proteins. (B) Poly(A)$^+$ RNA from MCA3D (lane 1), PDV (lane 2), HaCa4 (lane 3) and NIH 3T3 (lane 4) cells were subjected to RT-PCR with OTS-8 (upper panel) or β-actin (lower panel) oligonucleotides. (C) Nucleotide sequence of PA2.26 cDNA and amino acid sequence of the encoded protein. The two peptides originally identified by microsequencing are underlined. The putative membrane-spanning domain is shaded. Accession number: AJ250246 (EMBL).

density (Fig. 8C, right). Confocal imaging of cells doubly stained with phalloidin or anti-ezrin antibody and mAb PA2.26 revealed a gross perturbation of the actin cytoskeleton in PA2.26 transfectants (Fig. 9). Phalloidin staining in MCA3D and control clone 3DN5 showed the presence of strong cortical actin bundles and stress fibers (Fig. 9A) that dissapeared in 3D2.26 transfectants (Fig. 9B). Phalloidin staining in these cells was diffuse and concentrated at the cell periphery in projections and ruffles that emerged from the lateral surfaces at cell-cell boundaries, where a clear colocalization between actin filaments and PA2.26 antigen was observed (Fig. 9B,C, arrowhead). On the other hand, ezrin was distributed as a punctate staining throughout (underneath) the plasma membrane in the parental cells and control clones (Fig. 9D), while in 3D2.26 transfectants it was concentrated with PA2.26 in filopodia and ruffles (Fig. 9E,F, arrows and arrowheads, respectively). No differences in the level of expression of ezrin were observed between the control and 3D2.26 cells, as ascertained by western immunoblotting (data not shown).

To test whether the observed phenotypic changes in 3D2.26 transfectants correlated with increased motility, we used a wound healing assay in which the abilities of the cell lines to repopulate a wound made in confluent cultures were compared. As shown in Fig. 10, only a few cells from MCA3D and control clones were able to migrate but remained very close to the wound lining (Fig. 10A,C,E). In contrast, a substantial proportion of 3D2.26 transfectant cells invaded the empty area of the wound (Fig. 10B,D,E). This effect can not be attributed to increased proliferation, since no

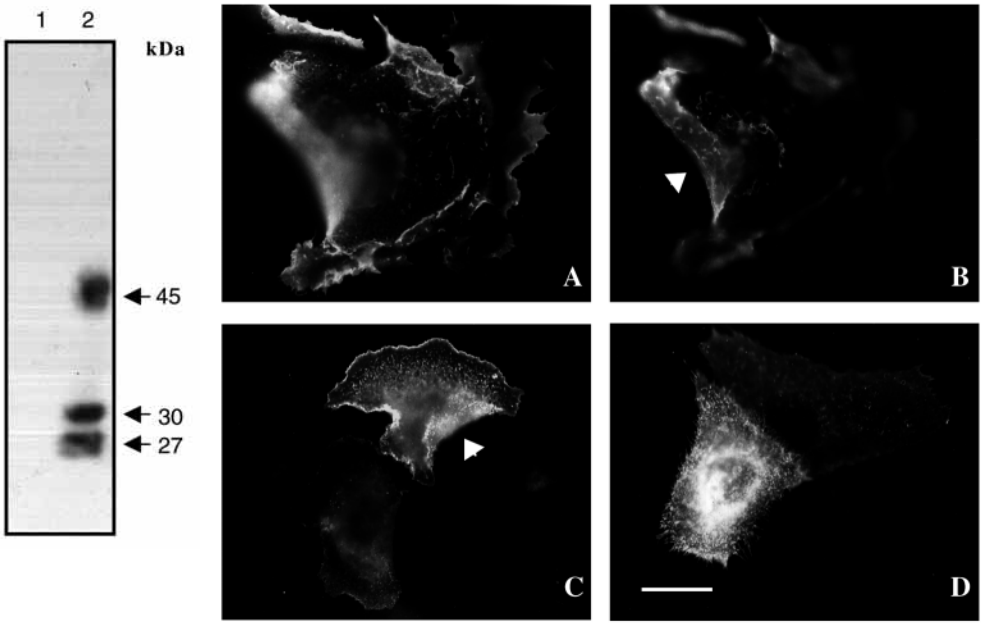

Fig. 7. Analysis of cells transiently transfected with the PA2.26 cDNA. In the left panel, the expression of PA2.26 protein in COS cells infected/transfected with the empty vector (lane 1) and PA2.26 cDNA (lane 2) is analyzed by western immunoblotting. The right panels present the immunofluorescent localization of PA2.26 in cell lines transiently transfected with PA2.26 cDNA. (A,B) COS; (C) MCA3D; (D) HaCaT. Images in A and B show the same field with the plane of focus adjusted at the bottom and the upper part of the cells, respectively. Arrowheads indicate prominent membrane ruffles. Bar, 10 μm.

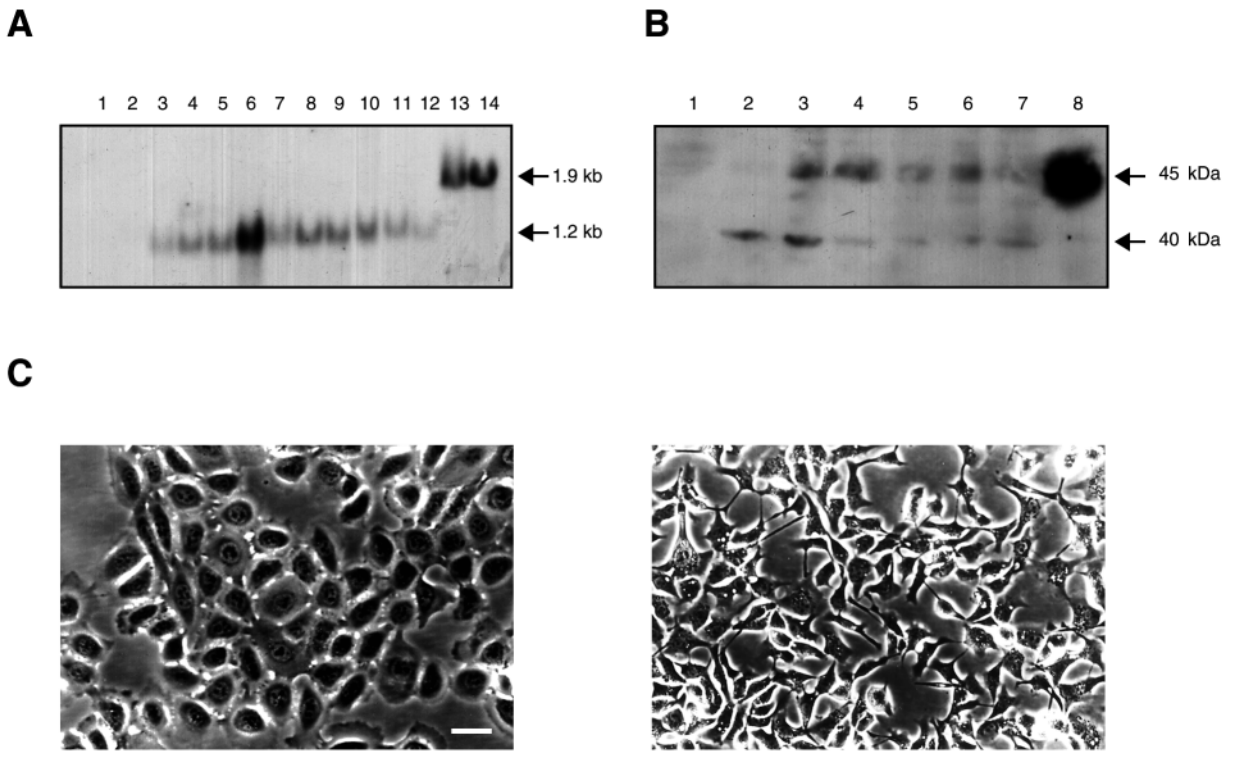

Fig. 8. Morphological change induced by stable transfection of PA2.26 cDNA into MCA3D keratinocytes. (A) Northern blot analysis of PA2.26 expression. Lane 1, parental MCA3D cells; lane 2, control clone 3DN5; lanes 3-12, PA2.26-transfected clones (3, 3D2.26-1; 4, 3D2.26-2; 5, 3D2.26-3; 6, 3D2.26-4; 7, 3D2.26-6; 8, 3D2.26-7; 9, 3D2.26-10; 10, 3D2.26-11; 11, 3D2.26-12; 12, 3D2.26-13); lane 13, PDV; lane14, HaCa4. 20 μg of total RNA was loaded per lane. (B) Western blot comparing the expression of PA2.26 protein in NIH3T3 and MCA3D cell transfectants. Lanes are: 1, 3DN5; 2, 3D2.26-1; 3, 3D2.26-2; 4, 3D2.26-3; 5, 3D2.26-4; 6, 3D2.26-6; 7, 3D2.26-11; 8, NIH3T3. Samples of cell extracts containing the same amount of protein (30 μg) were fractioned by 10% SDS-PAGE and immunoblotted with mAb PA2.26. (C) Phase-contrast micrographs of control clone 3DN5 (left) and a representative PA2.26-transfected clone: 3D2.26-2 (right). The rest of the 3D2.26 cell transfectant clones exhibit a similar morphology. Bar, 20 μm.

significant differences in growth properties (rather 3D2.26 clones exhibited a slightly slower rate of growth) were observed between 3DN and 3D2.26 cell lines (data not shown).

DISCUSSION

In this report we have identified and cloned a type I membrane mucin-like glycoprotein that localizes at cell surface projections of cultured mouse carcinoma cells and fibroblasts. This protein is recognized by mAb PA2.26, produced against transformed epidermal keratinocytes, and is induced during wound healing and skin carcinogenesis, as previously described (Gandarillas et al., 1997).

The amino acid sequence of PA2.26 antigen exhibits a high homology with two previously described mouse proteins, OTS-8 and gp38, identified as a phorbol ester-inducible gene in cultured osteoblasts and as a marker of stromal cells in T-cell dependent areas of peripheral lymphoid tissue, respectively (Nose et al., 1990; Farr et al., 1992). The rat (T1α/E11/podoplanin) and canine (gp40) homologs of murine OTS-8/gp38/PA2.26 have also been described by different groups (Rishi et al., 1995; Wetterwald et al., 1996; Breiteneder-Geleff et al., 1997; Zimmer et al., 1997). All of them synthesize type I transmembrane proteins of around 170 amino acids with highly homologous short cytoplasmic domains of nine residues, except for OTS-8 where a longer endodomain of 42 amino acids has been reported (Nose et al., 1990). The different mouse proteins are likely encoded by the same gene and discrepancies in the reported cDNA sequences, particularly the longer open reading frame reported for OTS-8 cDNA, are probably due to sequencing errors. In the rat, T1α sialoglycoprotein was first described as a marker of alveolar type I epithelial cells of the lung (Rishi et al., 1995). E11 antigen was found to be present in rat osteoblasts, osteocytes, alveoli, choroid plexuses and endothelia of lymphatic vessels (Wetterwald et al., 1996). Most recently, podoplanin has been identified in glomerular epithelial cells (podocytes) associated to a experimentally induced nephropathy (Breiteneder-Geleff et al., 1997). In the dog, gp40 was described as a major apical cell-surface sialoglycoprotein of type I MDCK cells (Zimmer et al., 1997). Although a role for canine gp40 as a receptor for influenza C virus has been proposed (Zimmer et al., 1995), and speculations about the participation of T1α in active ion transport and water fluxes were postulated (Williams et al., 1996), the function of all these proteins is unknown.

In this article, we present experimental evidence that points to an involvement of PA2.26 in the organization of the actin cytoskeleton in dynamic membrane structures associated with motility processes.

The actin cytoskeleton has been implicated in many cellular functions, including chemotaxis and motility (Condeelis, 1993;

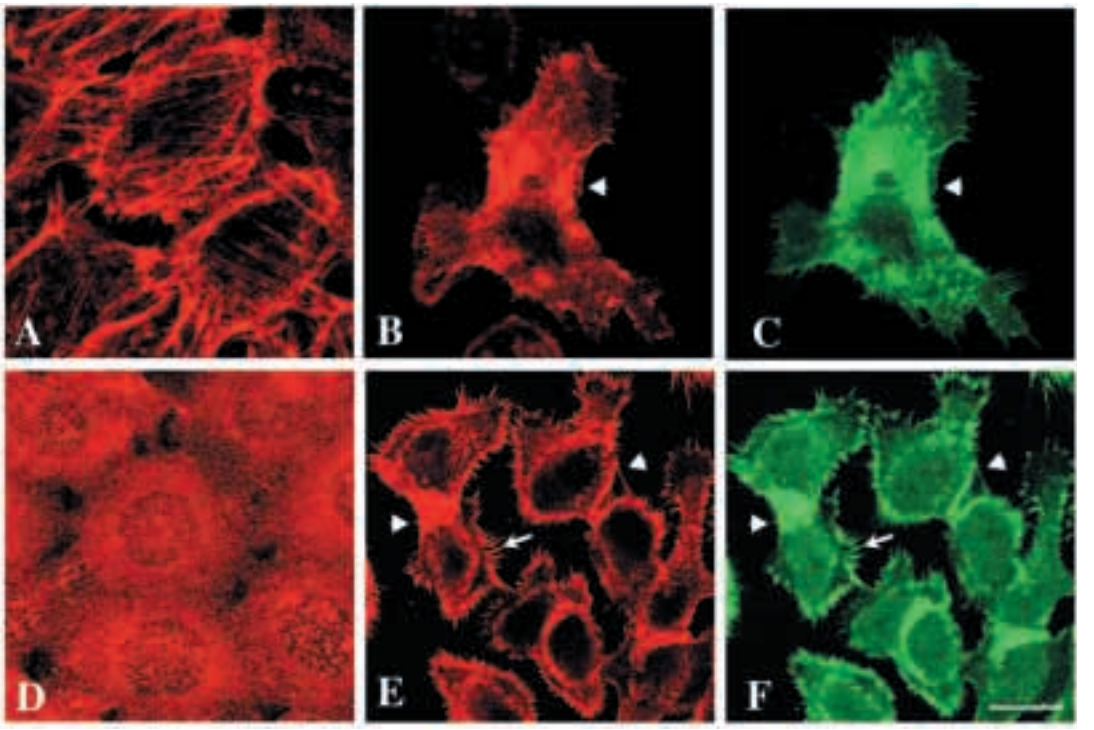

Fig. 9. Immunofluorescence colocalization of PA2.26 antigen with F-actin and ezrin in 3D2.26 cell transfectants. Control clone 3DN5 (A,D) was stained with phalloidin (A) and anti-ezrin polyclonal antibody (D). PA2.26-transfected clones 3D2.26-11 (B,C) and 3D2.26-4 (E,F), were doubly stained with phalloidin (B) and mAb PA2.26 (C) or anti-ezrin antibody (E) and mAb PA2.26 (F). All panels show confocal images. Arrowheads indicate ruffles formed between two adjacent cells and arrows mark filopodia. Bar, 10 μm.

Mitchison and Cramer, 1996). In epithelial cells, the precise organization of actin filaments is involved in cell-cell and cell-substratum adhesion and in the maintenance of cell shape (Gumbiner, 1996; Drubin and Nelson, 1996). Cell locomotion implies a change in the dynamic of cell surface with extension and retraction of plasma membrane projections (i.e. filopodia, lamellipodia and ruffles), mediated by the assembly and disassembly of actin filaments (Mitchison and Cramer, 1996; Welch et al., 1997).

PA2.26 is concentrated in actin-rich filopodia, lamellipodia and ruffles of cultured carcinoma and fibroblast cells, but seems to be excluded from stress fibers and cortical actin bundles involved in cell adhesion (Fig. 2). By electron microscopy, PA2.26 is found in other actin-rich structures as membrane microvilli (Fig. 3). Additional data from our laboratory (F. G. Scholl and M. Quintanilla, unpublished results) support this contention: PA2.26 was induced in serum-starved quiescent Swiss 3T3 cells by PMA and bradykinin, which promote the formation of ruffles and filopodia, respectively, but not by lysophosphatidic acid, which leads to the assembly of stress fibers and focal adhesion formation (Ridley and Hall, 1992; Ridley et al., 1992; Kozma et al., 1995).

Interestingly, PA2.26 colocalizes with ERM proteins in plasma membrane extensions of cultured cells (Fig. 2). Furthermore, the tissue distribution of PA2.26 (Fig. 5) coincides with that of either ezrin or moesin in the same type of cells and subcellular structures, although there are tissues where ezrin is strongly expressed and PA2.26 is absent, such as the intestinal epithelia. Notably, coinciding with PA2.26, ezrin has been found on the apical surface of epithelial cells of the choroid plexus and glomerulus, and on microvilli of mesothelia covering organs of the pleural, visceral and peritoneal cavities, while moesin is enriched in endothelial cells and in certain polarized epithelial cells such as that of alveoli (Berryman et al., 1993; Amieva et al., 1994; Schwartz-Albiez et al., 1995; Bohling et al., 1996). On the other hand, ezrin and moesin, but not radixin, were coimmunoprecipitated with PA2.26 from 1% Triton X-100 cell lysates, suggesting an association of these proteins in a complex inside the cells. Nevertheless, the association between PA2.26 and ezrin/moesin appeared to be weak since the complex was disrupted in a stronger lysis buffer (RIPA).

ERM proteins act as universal linkers between the actin cytoskeleton and integral proteins of the plasma membrane (i.e. CD44, CD43, ICAM-2) and appear to have a dynamic role in the formation and maintenance of cellular structures involving actin filaments, such as surface microvilli (Takeuchi et al., 1994; Tsukita et al., 1994; Helander et al., 1996; Yonemura et al., 1999), and in integrating signals elicited by motogenic/morphogenic growth factors in epithelial cells (Crepaldi et al., 1997). The regions of CD44, CD43 and ICAM-2 responsible for the binding to ERM proteins have been located in a juxta-membrane cluster of positively charged amino acids (Yonemura et al., 1998). The short cytoplasmic domain (KKISGRFSP) of PA2.26 contains three basic amino acids (two lysines and one arginine), whereas the rest are uncharged polar or nonpolar residues. The calculated isoelectric point of the whole domain is 11.17, indicating a net positive charge at neutral pH. This cluster of basic amino acids in the endodomain is shared by other transmembrane proteins of microvillal location such as 5T4 oncofetal antigen (Myers et al., 1994; Carsberg et al., 1995), L-selectin (Picker et al., 1991) and ICAM-1 (Carpén et al., 1992). However, the functional importance of the ERM-binding site for directing protein distribution at microvilli is unclear since mutation of the basic cluster has no effect on CD44 localization to membrane projections (Legg and Isacke, 1998). Experiments with gluthation-S-transferase-PA2.26 fusion constructs, and of site-directed mutagenesis, aimed at evaluating the direct interaction

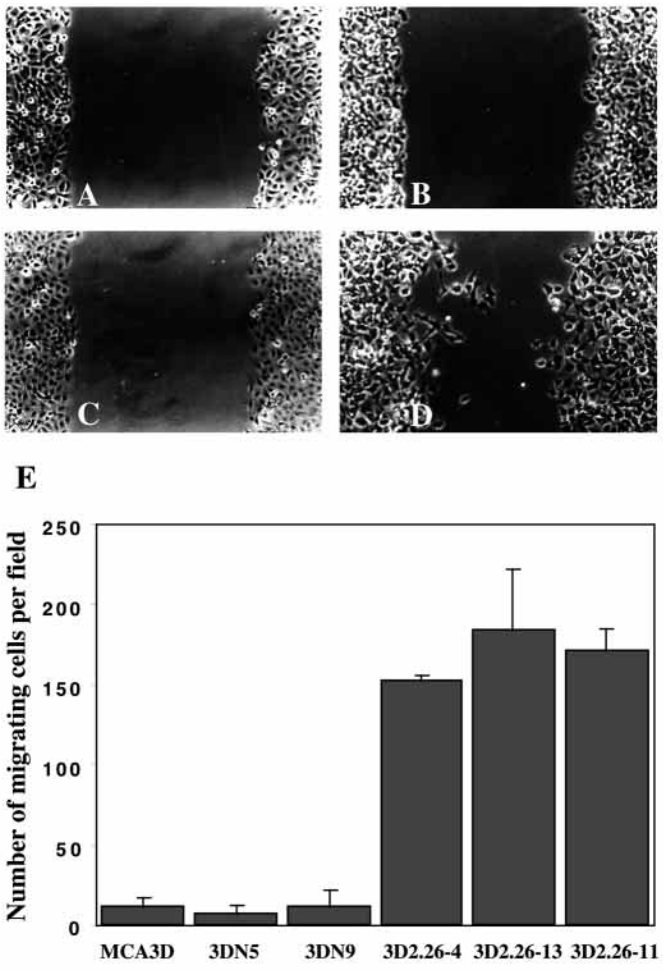

Fig. 10. Migration assay. Wounds made in confluent 3DN5 (A) and 3D2.26-4 (B) cell lines were examined after 24 hours of culture (C, 3DN5; D, 3D2.26-4). (E) Diagram showing quantification of the cell migration assay for the indicated cell lines. Cells invading the wound area were counted in 3-4 different fields (×20) from those shown in the micrographs. Values are means ± s.d.

of PA2.26 with recombinant ERM proteins and the importance of the endodomain in localization of the antigen at the plasma membrane, are currently in progress.

Biochemical characterization and nucleotide sequence prediction of PA2.26 reveal that it is a sialylated transmembrane glycoprotein with an ectodomain rich in serines and threonines. This extracellular domain has an extended and rigid structure with a net negative charge as a result of extensive O-glycosilation, characteristic of mucin-like glycoproteins (see Hilkens et al., 1992; Gendler and Spicer, 1995, for reviews). Increased levels of expression of membrane-associated mucins, such as episialin (MUC1) (Ligtenberg et al., 1990), epiglycanin (Kemperman et al., 1994) and sialomucin ASGP-1 (Carraway et al., 1992), have been linked to cancer and metastasis. Overexpression of episialin, epiglycanin and sialomucin in cultured cells inhibit cell-cell and cell-substratum adhesion (Kemperman et al., 1994; Wesseling et al., 1995, 1996; Komatsu et al., 1997). The anti-adhesive function of these mucins is a consequence of steric hindrance of cell adhesion receptors due to their large ectodomains consisting of repetitive mucin-like sequences. In contrast, based in the assumption that in a mucin-like domain 20-amino acids residues are approximately 5-nm long (Jentoft, 1990), the estimated size of PA2.26 ectodomain is 33 nm, a value that is in the range of cell adhesion receptors (Becker et al., 1989; Hynes, 1992).

Immortalized MCA3D keratinocytes are cohesive, nonmotile cells and show a characteristic actin cytoskeleton formed by strong cortical bundles and stress fibers (Caulín et al., 1995; Gómez et al., 1994-95; this paper). Transfection experiments show that expression of PA2.26 in MCA3D keratinocytes leads to alteration of cell-cell adhesion and induction of plasma membrane extensions and ruffles, concomitantly to a profound reorganization of the actin cytoskeleton and redistribution of ezrin to membrane projections (Fig. 9), indicating a change in the balance of forces within the cytoskeleton that control cell shape. Although transmembrane mucins alter cell shape and adhesion, the short ectodomain of PA2.26 rather indicates that the effects on the actin cytoskeleton and cell morphology can be mediated by the transmembrane and/or cytoplasmic domains. The fact that, in 3D2.26 transfectant cells, PA2.26 colocalizes with actin and ezrin in membrane extensions indicates that a physical association of PA2.26 with the actin cytoskeleton does indeed exist, and suggests a mechanism by which PA2.26 can induce a rearrangement of the actin cytoskeleton by recruitment of ERM proteins. Therefore, PA2.26 might act as a specialized membrane anchor for ERM proteins in the cells and tissues in which the antigen is present. Whether interaction of PA2.26 with ezrin and moesin is direct or indirect through an adaptor (see Mangeat et al., 1999) is presently unknown, although the presence of a cluster of basic residues on the cytoplasmic side next to the transmembrane domain favours the former possibility.

The observation that 3D2.26 cells exhibit enhanced motility properties (Fig. 10), and are tumorigenic upon injection in nude mice (F. G. Scholl, C. Gamallo and M. Quintanilla, manuscript in preparation) indicates an active role of PA2.26 in cell migration and tumorigenesis. Although the molecular mechanism for the phenotypic changes induced by expression of PA2.26 in MCA3D cells remains to be investigated, we speculate that they are mediated by the effects of PA2.26 on the cytoskeleton. Relocalization of ezrin to microvilli and ruffles is induced in epithelial cells stimulated by motility factors (Berryman et al., 1995) and functional inactivation of ezrin by dominant-negative mutants impairs growth factor-induced cell migration (Crepaldi et al., 1997). On the other hand, loss of the cortical actin network (Fig. 9) might account for destabilization of adherens junctions in 3D2.26 cells (F. G. Scholl, C. Gamallo and M. Quintanilla, manuscript in preparation). In support of this, it has been demonstrated that mechanical tension generated within the cytoskeleton can regulate cell shape and cause cells to switch between different genetic programs (Chicurel et al., 1998), and loss of cortical F-actin and destabilization of adherens junctions have been shown to contribute to tumor progression (Fischer and Quinlan, 1998).

We thank Drs Paul Mangeat and Ossi Turunen for their useful gifts of anti-ERM antibodies, Dr Norbert Fusenig for providing us with the HaCaT cell line, and Susanna Castel for her expert technical

assistance. We also thank Dr Francisco Wandosell for help with the glycosylation studies and Dr Amparo Cano for critical reading of the manuscript and helpful suggestions. This work was supported by grants 95-0177-OP of 'Programa de Estímulo a la Transferencia de Resultados de Investigación' (PETRI) and SAF98-0085-CO3-02 from the 'Comisión Interministerial de Ciencia y Tecnología' (CICYT) of Spain (to M.Q.), and by grant SAF98-0135 from the CICYT (to S.V.). F. G. Scholl is the recipient of a fellowship from the company Biosystems SA (Barcelona, Spain).

REFERENCES

Amieva, M. R., Wilgenbus, K. K. and Furthmayr, H. (1994). Radixin is a component of hepatocyte microvilli in situ. *Exp. Cell. Res.* **210**, 140-144.

Becker, J. W., Erickson, H. P., Hoffman, S., Cunningham, B. A. and Edelman, G. M. (1989). Topology of cell adhesion molecules. *Proc. Natl. Acad. Sci. USA* **86**, 1088-1092.

Berryman, M., Franck, Z. and Bretscher, A. (1993). Ezrin is concentrated in the apical microvilli of a wide variety of epithelial cells whereas moesin is found primarily in endothelial cells. *J. Cell Sci.* **105**, 1025-1043.

Berryman, M., Gary, R. and Bretscher, A. (1995). Ezrin oligomers are major cytoskeletal components of placental microvilli: a proposal for their involvement in cortical morphogenesis. *J. Cell Biol.* **131**, 1231-1242.

Bohling, T., Turunen, O., Jaaskelainen, J., Carpen, O., Sainio, M., Wahlstrom, T., Vaheri, A. and Haltia, M. (1996). Ezrin expression in stromal cells of capillary hemangioblastoma. An immunohistochemical survey of brain tumors. *Am. J. Pathol.* **148**, 367-373.

Bordier, C. (1981). Phase separation of integral membrane proteins in Triton X-114 solution. *J. Biol. Chem.* **256**, 1604-1607.

Boukamp, P., Petrusevska, R. T., Breitkreutz, D., Hornung, J., Markham, A. and Fusenig, N. E. (1988). Normal keratinization in a spontaneously immortalized aneuploid keratinocyte cell line. *J. Cell Biol.* **106**, 761-771.

Breiteneder-Geleff, S., Matsui, K., Soleiman, A., Meraner, P., Poczewski, H., Kalt, R., Schaffner, G. and Kerjaschki, D. (1997). Podoplanin, novel 43-kd membrane protein of glomerular epithelial cells, is downregulated in puromycin nephrosis. *Am. J. Pathol.* **151**, 1141-1152.

Brockhausen, I., Schutzbach, J. and Kuhns, W. (1998). Glycoproteins and their relationship to human disease. *Acta Anat.* **161**, 36-78.

Buchmann, A., Ruggeri, B., Klein-Szanto, A. J. P. and Balmain, A. (1991). Progression of squamous carcinoma cells to spindle carcinomas of mouse skin is associated with an imbalance of H-*ras* alleles on chromosome 7. *Cancer Res.* **51**, 4097-4101.

Carpén, O., Pallai, P., Staunton, D. E. and Springer, T. A. (1992). Association of intercellular adhesion molecule-1 (ICAM-1) with actin-containing cytoskeleton and alpha-actinin. *J. Cell Biol.* **118**, 1223-1234.

Carraway, K. L., Fregien, N., Carraway, K. L. and Carraway, C. A. (1992). Tumor sialomucin complexes as tumor antigens and modulators of cellular interactions and proliferation. *J. Cell Sci.* **103**, 299-307.

Carsberg, C. J., Myers, K. A., Evans, G. S., Allen, T. D. and Stern, P. L. (1995). Metastasis-associated 5T4 oncofoetal antigen is concentrated at microvillus projections of the plasma membrane. *J. Cell Sci.* **108**, 2905-2916.

Casaroli-Marano, R. P., Garcia, R., Vilella, E., Olivecrona, G., Reina, M. and Vilaró, S. (1998). Binding and intracellular trafficking of lipoprotein lipase and triacylglycerol-rich lipoproteins by liver cells. *J. Lipid Res.* **39**, 789-806.

Caulín, C., Scholl, F. G., Frontelo, P., Gamallo C. and Quintanilla, M. (1995). Chronic exposure of cultured transformed mouse epidermal cells to transforming growth factor-β_1 induces an epithelial-mesenchymal transdifferentiation and a spindle tumoral phenotype. *Cell Growth Differ.* **6**, 1027-1035.

Chicurel, M. E., Chen, C. S. and Ingber, D. E. (1998). Cellular control lies in the balance of forces. *Curr. Opin. Cell Biol.* **10**, 232-239.

Condeelis, J. (1993). Life at the leading edge: the formation of cell protrusions. *Annu. Rev. Cell Biol.* **9**, 411-444.

Crepaldi, T., Gautreau, A., Comoglio, P. M., Louvard, D. and Arpin, M. (1997). Ezrin is an effector of hepatocyte growth factor-mediated migration and morphogenesis in epithelial cells. *J. Cell Biol.* **138**, 423-434.

Drubin, D. G. and Nelson, W. J. (1996). Origins of cell polarity. *Cell* **84**, 335-344.

Farr, A. G., Berry, M. L., Kim, A. Nelson, A. J., Welch, M. P. and Aruffo, A. (1992). Characterization and cloning of a novel glycoprotein expressed by stromal cells in T-dependent areas of peripheral lymphoid tissues. *J. Exp. Med.* **176**, 1477-1482

Fischer, R. S. and Quinlan, M. P. (1998). Identification of a novel mechanism of regulation of the adherens junction by E1A, Rac1 and cortical actin filaments that contributes to tumor progression. *Cell Growth Differ.* **9**, 905-918.

Gandarillas, A., Scholl, F. G., Benito, N., Gamallo, C. and Quintanilla, M. (1997). Induction of PA2.26, a cell-surface antigen expressed by active fibroblasts, in mouse epidermal keratinocytes during carcinogenesis. *Mol. Carcino.* **20**, 10-18.

García-Gallo, M., Behrens, M., Renart, J. and Díaz-Guerra, M. (1999). Expression of N-methyl-D-aspartate receptors using vaccinia virus causes excitotoxic death in human kidney cells. *J. Cell. Biochem.* **72**, 135-144.

Gendler, S. J. and Spicer, A. P. (1995). Epithelial mucin genes. *Annu. Rev. Physiol.* **57**, 607-634.

Gómez, M., Navarro, P. and Cano, A. (1994-95). Cell adhesion and tumor progression in mouse skin carcinogenesis: increased synthesis and organization of fibronectin is associated with the undifferentiated spindle phenotype. *Invasion Metastasis* **14**, 17-26.

Gumbiner, B. M. (1996). Cell adhesion: the molecular basis of tissue architecture and morphogenesis. *Cell* **84**, 345-357.

Helander, T. S., Carpen, O., Turunen, O., Kovanen, P. E., Vaheri, A. and Timonen, T. (1996). ICAM-2 redistributed by ezrin as a target for killer cells. *Nature* **382**, 265-268.

Hilkens, J., Ligtenberg, M. J. L., Vos, H. L. and Litvinov, S. V. (1992). Cell membrane-associated mucins and their adhesion-modulating property. *Trends Biochem. Sci.* **17**, 359-363.

Hynes, R. O. (1992). Integrins: versatility, modulation, and signaling in cell adhesion. *Cell* **69**, 11-25.

Jentoft, N. (1990). Why are proteins O-glycosylated? *Trends Biochem. Sci.* **15**, 291-294

Kemperman, H., Wijnands, Y., Wesseling, J., Niessen, C. M., Sonnenberg, A. and Roos, E. (1994). The mucin epiglycanin on TA3/Ha carcinoma cells prevents alpha 6 beta 4-mediated adhesion to laminin and kalinin and E-cadherin-mediated cell-cell interaction. *J. Cell Biol.* **127**, 2071-2080.

Komatsu, M., Carraway, C. A., Fregien, N. L. and Carraway, K. L. (1997). Reversible disruption of cell-matrix and cell-cell interactions by overexpression of sialomucin complex. *J. Biol. Chem.* **272**, 33245-33254.

Kozma, R., Ahmed, S., Best, A. and Lim, L. (1995). The ras related protein Cdc42Hs and bradykinin promote formation of peripheral actin microspikes and filopodia in Swiss 3T3 fibroblasts. *Mol. Cell. Biol.* **15**, 1942-1952.

Legg, J. W. and Isacke, C. M. (1998). Identification and functional analysis of the ezrin-binding site in the hyaluronan receptor, CD44. *Curr. Biol.* **8**, 705-708.

Ligtenberg, M. J., Vos, H. L., Gennissen, A. M. and Hilkens, J. (1990). Episialin, a carcinoma-associated mucin, is generated by a polymorphic gene encoding splice variants with alternative amino termini. *J. Biol. Chem.* **265**, 5573-5578.

Mangeat, P., Roy, C. and Martin, M. (1999). ERM proteins in cell adhesion and membrane dynamics. *Trends Cell Biol.* **9**, 187-192.

Mitchison, T. J. and Cramer, L. P. (1996). Actin-based cell motility and cell locomotion. *Cell* **84**, 371-379.

Myers, K. A., Rahi-Saund, V., Davison, M. D., Young, J. A., Cheater, A. J. and Stern, P. L. (1994). Isolation of a cDNA encoding 5T4 oncofetal trophoblast glycoprotein. An antigen associated with metastasis contains leucine-rich repeats. *J. Biol. Chem.* **269**, 9319-9324.

Nose, K., Saito, H. and Kuroki, T. (1990). Isolation of a gene sequence induced later by tumor-promoting 12-O-tetradecanoylphorbol-13-acetate in mouse osteoblastic cells (MC3T3-E1) and expressed constitutively in ras-transformed cells. *Cell Growth Differ.* **1**, 511-518.

Pagan, R., Martin, I., Alonso, A., Llobera, M. and Vilaró, S. (1996). Vimentin filaments follow the preexisting cytokeratin network during epithelial-mesenchymal transition of cultured neonatal rat hepatocytes. *Exp. Cell Res.* **222**, 333-344.

Palacios, J. and Gamallo, C. (1998). Mutations in the β-catenin gene (*CTNNB1*) in endometrioid ovarian carcinomas. *Cancer Res.* **58**, 1344-1347.

Picker, L. J., Warnock, R. A., Burns, A. R., Doerschuk, C. M., Berg, E. L. and Butcher, E. C. (1991). The neutrophil selectin LECAM-1 presents carbohydrate ligands to the vascular selectins ELAM-1 and GMP-140. *Cell* **66**, 921-933.

Ridley, A. J. and Hall, A. (1992). The small GTP-binding protein rho regulates the assembly of focal adhesions and actin stress fibers in response to growth factors. *Cell* **70**, 389-399.

Ridley, A. J., Paterson, H. F., Johnston, C. L., Diekmann, D. and Hall, A.

(1992). The small GTP-binding protein rac regulates growth factor-induced membrane ruffling. *Cell* **70**, 401-410.

Rishi, A. K., Joyce-Brady, M., Fisher, J., Dobbs, L. G., Floros, J., Van der Spek, J., Brody, J. S. and Williams, M. C. (1995). Cloning, characterization, and development expression of a rat lung alveolar type I cell gene in embryonic endodermal and neural derivatives. *Dev. Biol.* **167**, 294-306.

Schwartz-Albiez, R., Merling, A., Spring, H., Moller, P. and Koretz, K. (1995). Differential expression of the microspike-associated protein moesin in human tissues. *Eur. J. Cell Biol.* **67**, 189-198.

Takeuchi, K., Sato, N., Kasahara, H., Funayama, N., Nagafuchi, A., Yonemura, S., Tsukita, Sa. and Tsukita, Sh. (1994). Perturbation of cell adhesion and microvilli formation by antisense oligonucleotides to ERM family members. *J. Cell Biol.* **125**, 1371-1384.

Tsukita, Sa., Oishi, K., Sato, N., Sagara, J., Kawai, A. and Tsukita, Sh. (1994). ERM family members as molecular linkers between the cell surface glycoprotein CD44 and actin-based cytoskeletons. *J. Cell Biol.* **126**, 391-401.

Tsukita, Sa., Yonemura, S. and Tsukita, Sh. (1997). ERM (ezrin/radixin/moesin) family from cytoskeleton to signal transduction. *Curr. Opin. Cell Biol.* **9**, 70-76.

Varki, A. (1994). Selectin ligands. *Proc. Natl. Acad. Sci USA* **91**, 7390-7397.

Welch, M. D., Mallavarapu, A., Rosenblatt, J. and Mitchison, T. J. (1997). Actin dynamics in vivo. *Curr. Opin. Cell Biol.* **9**, 54-61.

Wesseling, J., van der Valk, S. W., Vos, H. L., Sonnenberg, A. and Hilkens, J. (1995). Episialin (MUC1) overexpression inhibits integrin-mediated cell adhesion to extracellular matrix components. *J. Cell Biol.* **129**, 255-265.

Wesseling, J., van der Valk, S. W. and Hilkens, J. (1996). A mechanism for inhibition of E-cadherin-mediated cell-cell adhesion by the membrane-associated mucin episialin/MUC1. *Mol. Biol. Cell.* **7**, 565-577.

Wetterwald, A., Hoffstetter, W., Cecchini, M. G., Lanske, B., Wagner, C., Fleisch, H. and Atkinson, M. (1996). Characterization and cloning of the E11 antigen, a marker expressed by rat osteoblasts and osteocytes. *Bone* **18**, 125-132.

Williams, M. C., Cao, Y., Hinds, A., Rishi, A.K. and Wetterwald, A. (1996). T1α protein is developmentally regulated and expressed by alveolar type I cells, choroid plexus, and ciliary epithelia of adult rats. *Am. J. Respir. Cell Mol. Biol.* **14**, 577-585.

Yonemura, S., Hirao, M., Doi, Y., Takahashi, N., Kondo, T., Tsukita, Sa. and Tsukita, Sh. (1998). Ezrin/radixin/moesin (ERM) proteins bind to a positively charged amino acid cluster in the juxta-membrane cytoplasmic domain of CD44, CD43, and ICAM-2. *J. Cell Biol.* **140**, 885-895.

Yonemura, S., Tsukita, Sa. and Tsukita, Sh. (1999). Direct involvement of Ezrin/Radixin/Moesin (ERM)-binding membrane proteins in the organization of microvilli in collaboration with activated ERM proteins. *J. Cell Biol.* **145**, 1497-1509.

Zimmer, G., Klenk, H. D. and Herrler, G. (1995). Identification of a 40-kDa cell surface sialoglycoprotein with the characteristics of a major influenza C virus receptor in a Madin-Darby canine kidney cell line. *J. Biol. Chem.* **270**, 17815-17822.

Zimmer, G., Lottspeich, F., Maisner, A., Klenk, H. D. and Herrler, G. (1997). Molecular characterization of gp40, a mucin-type glycoprotein from the apical plasma membrane of Madin-Darby canine kidney cells (type I). *Biochem. J.* **326**, 99-108.